Proceedings of the 21st ICSMGE, Vienna, Austria, 14 – 19 June 2026. Pistrol, Adam & Schweiger (eds.)
Published by: ÖGG, Austrian Society for Geomechanics, Salzburg, Austria, ISBN 978-3-9503898-4-5
https://doi.org/10.53243/ICSMGE2026-1417

Safe and economical geotechnical design of wind farm foundations in seismic areas based on a project from the USA and Romania

G. Allen Bowers, Jr., Ph.D., P.E., M.ASCE, Andrzej Wolski, Łukasz Ledziński,
Geopier, A Division of CMC, Davidson, NC, USA, allen.bowers@cmc.com

ABSTRACT: Climate change is spurring the transition from power generated by fossil fuels to power generated by wind, solar, and nuclear systems. These developments are often constructed at sub-optimal sites that face geotechnical and geologic hazards requiring mitigation for operational resiliency. This paper presents the results of an extensive ground improvement program applied at two projects: I phase of 72-turbine wind power project in Buzau, Romania (project A) and a 41-turbine wind power project in the Mississippi River Delta, USA (project B). Both sites are subject to significant seismic demand from the nearby Vrancea Seismic Zone (VSZ) and New Madrid Seismic Zone (NMSZ) respectively and contain loose alluvial soil that is susceptible to soil liquefaction when loaded to the design Peak Ground Accelerations (PGA) of up to 0.50g. The ground improvement system was required to mitigate liquefaction-induced settlements of up to 15cm, which would render the turbines inoperable. Further, the design seismically-induced shear stresses would result in significant soil shear strength reduction and lead to bearing instability. This paper discusses the design methods used to provide a robust and economical solution and summarizes the results of the post-installation CPT soundings used to verify performance. This paper is of particular importance because it provides a design framework for the effective treatment of Romanian and Central United States soil liquefaction when loaded to VSZ and NMSZ motions, an effort that resulted in greatly improved geotechnical performance and resiliency.

KEYWORDS: Rammed Aggregate Piers, liquefaction, Geopier's 3-step method.

1 INTRODUCTION

The transition from traditional fossil fuels to renewable energy sources is a critical component of global efforts to combat climate change. Two wind energy projects exemplify this shift by leveraging regional wind resources to deliver clean electricity at scale.

The first phase of the first project, denoted as project A and situated in Romania, involves the design and installation of 30 wind turbines. This wind project is expected to produce up to 192 Megawatts of electricity, supplying clean energy to around 110,000 homes and cutting CO_2 emissions by about 225,000 tons per year.

The second project, denoted as project B is located in the Mississippi River Delta, and utilizes 41 wind turbines to harness the area's natural wind potential. This project is designed to generate up to 200 Megawatts of electricity - enough to power nearly 80,000 homes while reducing carbon emissions by approximately 450,000 tons annually.

Project A is located near the Vrancea Seismic Zone (VSZ), one of Europe's most active seismic areas. While the site benefits from consistent wind patterns across open terrain, it also faces significant geotechnical challenges due to its proximity to a region known for intermediate-depth earthquakes.

Similarly, project B takes advantage of the region's ample wind currents while minimizing disruption to the predominately agricultural land use. However, the delta's geological setting presents its own difficulties due to the site's composition of primarily soft alluvial soils and 100 mile proximity to the New Madrid Seismic Zone (NMSZ). The soils are highly susceptible to liquefaction during seismic events due to the combination of the loose alluvial sandy and silty soils with the relatively high NMSZ ground motions, which could lead to excessive liquefaction-induced settlements that may compromise turbine performance.

This paper focuses on the comprehensive ground improvement program designed to mitigate the risks from liquefaction-induced settlements, which can be used as a framework for the effective treatment of soils prone to liquefaction to ultimately achieve greater geotechnical performance and resiliency.

Note that the ground improvement program was designed to meet additional static and seismic performance criteria for both projects including bearing capacity, rotational stability, and differential settlement among others. However, due to its chief role in design and the space limitations of this paper, the focus of this paper is solely on the ground improvement design for managing liquefaction induced settlements.

2 PROJECTS DETAILS

2.1 *Turbine types and performance requirements*

Project A utilizes Vestas V162-6.4 MW turbines with a 166-meter hub height, significantly increasing structural loads and design demands. Each turbine is founded on a circular mat foundation with a diameter of approximately 29.8 meters, embedded about 4.0 meters below finished grade. These foundations were structurally designed to resist overturning moments ranging from 155 to 193 MN-m, reflecting the increased height and power output of the turbines.

Project B incorporated Vestas V150 wind turbine generators with a 136-meter hub height, each mounted on a circular mat foundation embedded approximately 4.3 meters below final grade. The mat foundations ranged from 23.6 meters to 25.9 meters in diameter and were structurally designed to resist overturning moments between 105 and 150 MN-m.

Both projects include specific performance requirements with respect to static and post-seismic differential settlements of 3 mm/m and required dynamic rotational stiffness of 100 GN- m/rad.

2.2 *Geologic information*

Project A is situated in the Romanian Plain, a region developed atop the northern Moesian Platform through a sequence of Quaternary fluvial and lacustrine processes influenced by tectonic shifts, climatic cooling, and sediment influx from the Carpathians and the Danube. Subsurface exploration included both borehole drilling and cone penetration testing (CPT) at each turbine location. Typically, the soil profile consisted of 5 to 8 meters of silty gravel or silty sand overlying layers of clay and silty sand. The alluvial clays and silts exhibited medium stiff to stiff consistency, while the sands ranged from medium

dense to very dense. Groundwater levels varied across the site, generally appearing between 0.8 and 3.0 meters below the existing surface.

Ground improvement measures were implemented at 23 of the 30 turbine sites, but this paper focuses specifically on one location—Turbine A—for several key reasons. Although other turbines experienced greater liquefaction-induced settlement or lower factors of safety for bearing capacity in unimproved conditions, this site presented both issues and therefore required targeted mitigation. Additionally, Turbine A was selected for additional post-installation verification testing, providing a valuable data point for evaluating ground improvement effectiveness.

Figure 1 illustrates the subsurface profile at Turbine A, which includes predominantly fine-grained soils in the upper 5 meters, transitioning to loose coarse-grained material between 5 and 9.5 meters, and then to stiff clay at greater depth.

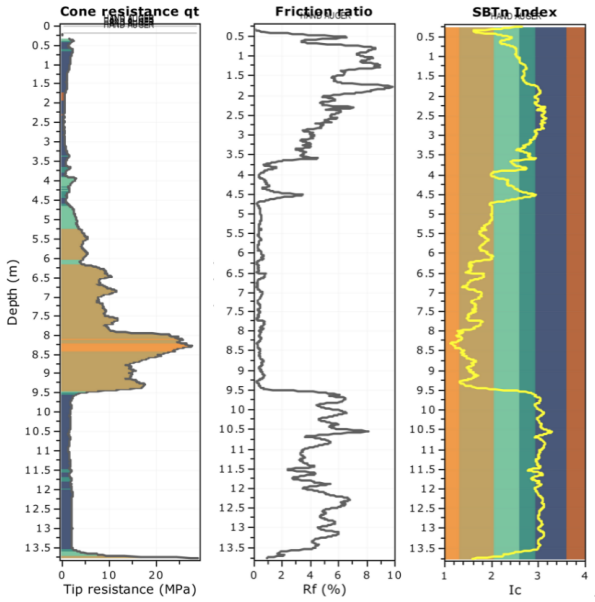

Figure 1. Cone resistance, friction ratio, and SBTn at Turbine A.

Project B is located at The Mississippi Alluvial Plain and the total project site area encompasses approximately 7,500 acres. Extensive historical and ongoing sediment deposition from the Mississippi River and its tributaries have created deep alluvial deposits that are highly variable in soil composition. The subsurface investigations conducted by the Geotechnical Engineer of Record (GEOR) consisted of both borings and CPTs at each turbine location. Generally, the subsurface consisted of 6 to 9 m of clay and silt underlain by sand and gravelly sand. The alluvial clay and silt were generally medium stiff to stiff in consistency and sands were generally medium dense to very dense. Groundwater was encountered at various depths across the project site, but generally ranged between 0.3 and 3.6 m below existing ground surface.

Although ground improvement was performed at 40 of the 41 turbine locations, this paper focuses on one of the turbine sites, denoted as Turbine B, for several reasons. First, though other sites had higher PGAs, more liquefaction-induced settlements, and/or lower unimproved bearing capacity factors of safety, this site required mitigation for each. Second, this was one of several sites selected to collect post-improvement data and thus the design can be verified.

Figure 2 shows the stratigraphy at Turbine B. The upper 10 m are primarily fine-grained with some lenses of coarser grain material around depths of 3 m and 6 m. At a depth of 10 m the profile transitions to loose, coarse grain material and becomes progressively denser with depth. Of important note is approximately 1.5 m layer of very soft slab material at a depth of about 8 m.

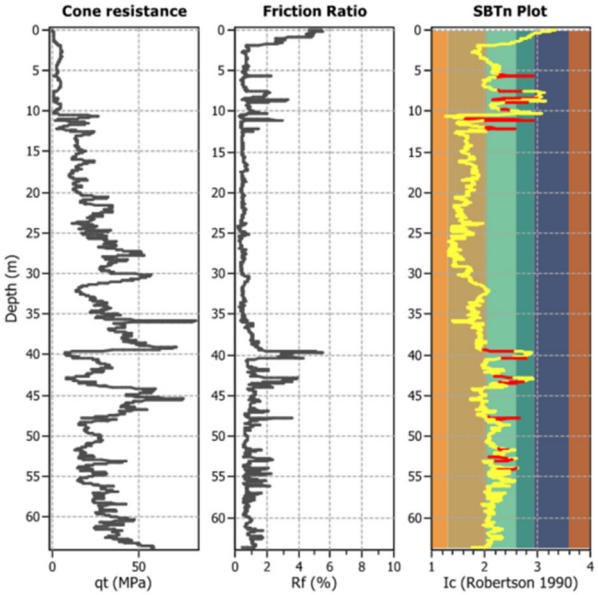

Figure 2. Cone resistance, friction ratio, and SBTn at Turbine B.

2.3 *Seismic conditions*

At Turbine A liquefaction analysis considers Peak Ground Acceleration (PGA) of 0.50 g in conjunction with a Mw=7.5 design earthquake event.

At Turbine B, the GEOR performed site-specific seismic response analyses, which included 5 ground motions from the PEER Ground Motion Database (NGA East). The GEOR recommended that liquefaction analyses consider a site-specific scaled PGA value in conjunction with a Mw=7.5 design earthquake event. The design PGA at Turbine B is 0.20 g.

The soils at many of the turbine locations for both projects are subject to liquefaction upon seismically-induced shear stresses. The potential for soil liquefaction triggering was estimated at each wind turbine location using the site-specific PGA in combination with the deep CPT soundings performed at each site. Liquefaction triggering was computed using the NCEER (Youd et al. 2001) procedures. Ic was calculated following the Robertson and Wride (1998) method as recommended by Robertson (2009) while also considering the influence of transition layers. The free-field post-liquefaction settlement for each liquefiable turbine site was determined in accordance with Zhang (2002). Settlement induced by liquefiable layers at deeper depths was accounted for in accordance with Cetin et al. (2009), by using a depth weighting factor of 1 at the ground surface, which decreases linearly to 0 at a depth of 18 meters.

3 GROUND IMPROVEMENT PROGRAM

In order to satisfy the performance criteria presented in paragraph 2.1, the design team selected Geopier Rammed Aggregate Piers (RAPs). RAPs are constructed by applying direct vertical compaction energy to successive layers of high-quality angular gravel. The vertical compaction serves to significantly reduce the void ratio resulting in densely compacted aggregate and a pier with a relatively high stiffness. The stiffness of the pier element is typically ten to forty times greater than that of the native soils (HITEC 2007).

Ground improvement programs, including ones that utilize RAPs, necessarily require design methods, performance criteria, and validation approaches that are understood and agreed upon by the ground improvement designer, installer, and project team. This section discusses the design framework that was used for this project. The design framework with respect to only one performance criteria, differential settlement, is discussed as this was the governing performance criteria for both projects with respect to the ground improvement design.

Both projects specified a static + seismic differential settlement tolerance of 3 mm/m. The unimproved and improved values for the turbines are summarized in Table 1 and explained in the following section.

Table 1. Summary of unimproved and improved performance criteria

Turbine	Performance criteria	unimproved	improved
A	*Differential settlements mm/m*	4.5	1.9
B		3.1	1.7

Note: Improved values refer to Geopier assigned design values. Improved values calculated from post-construction field validation testing are discussed in a subsequent section.

3.1 *Calculating static differential settlement in RAP-improved soil*

RAP elements control foundation settlements by increasing the composite elastic modulus of the ground. The composite vertical stiffness of the upper zone soil, E_{comp}, is a weighted average of the elastic pier stiffness and the matrix soil stiffness. E_{comp} is computed using the expression:

$$E_{comp} = E_g R_a + E_m(1 - R_a) \quad (1)$$

Where E_g is the RAP stiffness, R_a is the area replacement ratio, and E_m is the matrix soil stiffness. For soils with layers of varying stiffness values, which also directly affects the RAP stiffness values, the above expression can be used to determine an E_{comp} for each representative soil layer through which the RAP extends.

The settlement, s, for each layer, i, is a function of the composite layer stiffness, thickness of the layer, and stress increase to the layer. Layer settlement is provided by:

$$s_i = \frac{\Delta q_i H_i}{E_{comp,i}} \quad (2)$$

Where Δq is the change in stress of the layer i, and H is the thickness of the layer.

The portion of the profile consisting of improved ground is referred to as the upper zone UZ. The lower zone LZ is the unimproved portion of the profile beneath the reinforced zone, as shown in Figure 3.

The settlement of the lower zone is calculated using conventional geotechnical methods. The lower zone settlement is added to the upper zone settlement to determine the total settlement at a given point beneath the footprint of the structure.

Differential settlement occurs at wind turbines as they are loaded eccentrically from the wind itself. Representative load distributions were applied in Settle3 (Rocscience 2023) to produce stress-increase vs depth plots at positions of maximum and minimum stresses. These stresses were then used in conjunction with Equations 1 and 2 to derive differential settlement estimates.

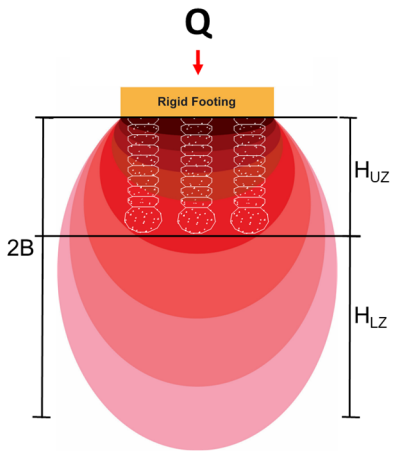

Figure 3. Improved upper zone UZ and lower zone LZ

3.2 *Calculating liquefaction-induced differential settlement in RAP-improved soil*

During liquefaction, RAPs provide three mechanisms that improve the liquefied performance of the supported structure (3-Step Method), which are densification, lateral stress stress increase, and the post-liquefaction stiffness of the RAPs. Each mechanism is explained in the subsequent sections.

3.2.1 *Densification*

The installation of the RAP elements densifies the native soils that are susceptible to densification (Majchrzak et al. 2009, Wissmann et al. 2015, Saftner et al. 2017, Vera-Grunauer et al. 2017, Amoroso et al. 2019, Rollins et al. 2021). For clean sand, pier spacings can often be designed considering the ground motion to provide post-installation SPT or CPT tip resistance values sufficient to render the soil non-liquefiable. For soils with higher fines content that are not as susceptible to densification such as silty sand and sandy silt, densification may still occur as measured by increases in SPT and CPT tip resistances, but these materials may not be improved to SPT- and CPT-based penetration resistances sufficient to result in a Factor of Safety (FS) greater than unity. In these soils, the other two methods of RAP liquefaction mitigation are more important.

3.2.2 *Lateral stress increase*

In addition to densification, the vertical compaction action of the RAP patented ramming tool compacts the aggregate laterally, causing it displace soil in the horizontal direction. The combination of the lateral compaction and cavity expansion increases lateral stress on the matrix soil. Liquefaction triggering is a mean effective stress phenomena (Harada et al. 2010) and therefore liquefaction triggering is mitigated by increasing the lateral and thus mean effective stress. Practically, this is realized as an increase in the cyclic resistance ratio (CRR) (Salgado et al. 1997). Amoroso et al. (2020) and Amoroso et al. (2024) directly measured the CRR increase factors (Km) resulting from the increase to the horizontal earth pressure coefficient, Ko, associated with the construction of RAPs through in-situ testing using the Dilatometer Test (DMT) and Cone Penetration Test (CPT). The results of the study suggest that Ko values in matrix soils increased by an average of 1.4, resulting in a Km coefficient value of 1.2. The effects of both densification and lateral stress increase on the CRR or cyclic stress ratio (CSR) are shown in Figure 4, below.

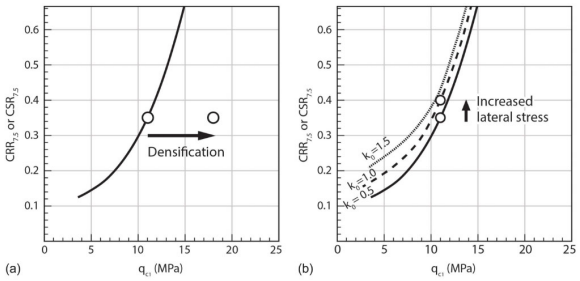

Figure 4. The effects of densification (a) and lateral stress increase (b) on the CRR and CSR (Amoroso et al. 2024).

3.2.3 *Post-liquefaction RAP stiffness*

The RAP element itself is both non-liquefiable and significantly stiffer than the in-situ soil. During a seismic event, the RAP element maintains much of its stiffness and thus serves to stiffen the overall soil profile and provide a reduction in the volumetric settlements associated with liquefaction. This has been observed in several, recent projects built with RAP elements, such as the Briceño embankment, Ecuador (Smith and Wissmann 2017, Vera-Grunauer, X.F. et al. 2019) and Emilia-Romagna, Italy (Amoroso et al. 2019, Amoroso et al. 2020). In both cases, densification and lateral stress increase alone were not able to account for the observed reduction in total liquefaction settlement. To account for the additional settlement reduction, Rollins et al. (2021) propose the use of the RAP elastic modulus to account for the improved performance and suggests that up to approximately 70 percent of the static RAP stiffness is maintained during liquefaction. For the wind turbine projects discussed herein, a post-liquefied elastic modulus of 100-120 MPa was used for the RAP elements, which is conservatively about 50 percent of the static RAP stiffness in these profiles.

3.3 *RAP design*

Considering the static and seismic design methodologies above, a RAP layout for Turbine A was designed in a radial geometry beneath the turbine with piers spaced on an average center-to-center spacing of 1.8 m and installation depth of 10.0 m below ground surface. The foundation was approximately 4 m below ground surface, thus resulting in RAP elements of 6.0 m after excavating to bottom of foundation.

A similar configuration was adopted for Turbine B, maintaining the radial pattern but increasing the pier spacing to 2.1 m and reducing the installation depth to 11.3 m. With a similar foundation embedment of approximately 4.2 m, this approach yielded RAP elements extending 7.1 m below the excavation level.

4 GROUND IMPROVEMENT DESIGN VALIDATION

Following installation on the ground improvement elements, field validation testing was performed to demonstrate the performance of the RAP elements. Field validation testing consisted of single element modulus tests to demonstrate the element static stiffness values and CPT soundings to record any increase in tip resistance with depth. The CPT soundings are more critical with respect to seismic performance as they demonstrate one of the three mechanisms of seismic improvement: densification.

4.1 *Turbine A*

Figure 5a, below, shows the CPT tip resistances vs depth for the unimproved profile (before RAP installation) and improved profile. There are two plots for the improved value representing two post CPTs done on both sides of pre CPT, each at approximately 6.0m distance and both reaching refusal at depth of 6-7m from the grade. Both post CPTs taken approximately 1.0m from a RAP element.

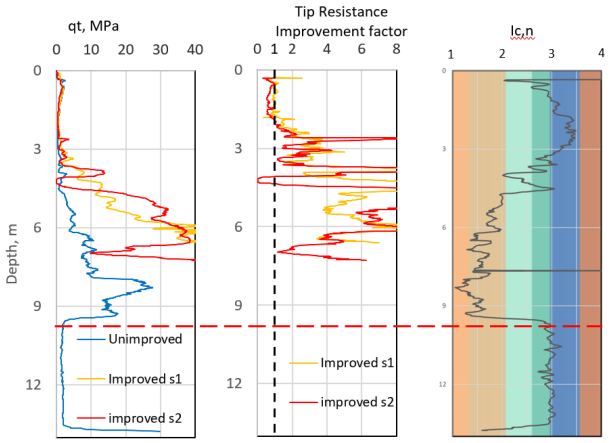

Figure 5. Pre and Post-CPT soundings (a, left); Tip resistance improvement (b, middle); Ic of pre-CPT (c, right). Depth of RAP elements indicated with dashed line

Both post-installation CPT soundings showed a marked increase in tip resistance versus the unimproved profile. The tip resistance improvement factor is shown in Figure 5b, which is the ratio of the post-installation CPT to the pre-installation CPT. From Figure 5b, several observations can be made. First, both post CPTs show similar improvement and reached refusal at similar depth which gives confidence that the same effect has been achieved across the foundation footprint.

Second, the improvement factor is generally close to 1 in the upper 2 m which is not surprising given Ic plot (Figure 5c) suggesting top 4 m to be more fine grained. On the contrary, we can see improvement factor increasing to about 2.5 at the depth of 3-4 m which should be attributed to the transition zone between fine grained and loose coarse-grained, hence densifiable material. At the depth of 4-6 m, where we have loose to medium dense silty sands, the improvement factor increases up to 5-6. While certainly beneficial, this amount of improvement is higher than what is typically observed in silty sands. The reasons for this degree of improvement are likely a combination of the facts that the soil may not be as silty as the CPTs suggest and thus additional grain sizes and hydrometer testing would be valuable; there is some difference in the fines content of the pre and post-improved CPT locations; and that the post-CPTs were not performed in the exact center between RAPs but closer to the constructed elements. Nevertheless, the post CPTs are more than satisfactory to meet the performance specifications.

It can also be noted that RAPs were arranged in a relatively dense layout of 1.8 m center to center. At 6-7 m depth the CPT refusal is anticipated. Ultimately the upper 3 m are inconsequential for this project because they are both above the groundwater elevation (non-liquefiable) and above the turbine foundation depth. The improvement factor of 5-6 below the foundation base level exceeds the design assumptions.

4.2 *Turbine B*

Similarly, Figure 6a, below, shows the CPT tip resistances vs depth for the unimproved and improved profile. There are two plots for the improved value – one for a sounding taken in the center of four RAP elements, resulting in a distance of 1.5 m from the nearest element, and one for a sounding taken 0.75 m from a RAP element.

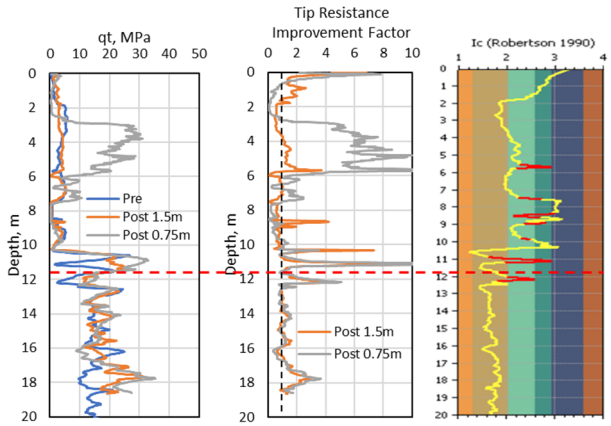

Figure 6. Pre and Post-CPT soundings (a, left); Tip resistance improvement (b, middle); Ic of pre-CPT (c, right). Depth of RAP elements indicated with dashed line

Both post-installation CPT soundings showed a marked increase in tip resistance versus the unimproved profile. The tip resistance improvement factor is shown in Figure 6b. From Figure 6b, several observations can be made. First, the CPT post-installation sounding conducted closer to the RAP element is similar to the one located directly between four elements, except for the depths between 3 and 6 m, in which the sounding closer to the RAP element displayed a higher degree of improvement. This indicates that for the given profile, the accumulated effects from four pier installations at a larger distance is roughly equivalent to the effect from a single pier installation at a closer distance at most depths.

Second, the improvement factor is generally between 1.5 and 2 (with an average of 2.2) in the upper 6 m, and then decreases to around 1, or slightly less than 1, between 6 and 10 m. This is expected as the Ic plot of the pre-installation CPT (Figure 6c) suggests that the material in these layers is more fine-grained and thus less susceptible to densification. Of particular interest is the zone between depths of 7.5 and 10 m, in which the improvement factor is less than 1 (average of 0.7). The Ic plots show this to be a very soft clay. The installation of the RAPs likely disturbed this clay layer resulting in lower post-CPT tip resistance values. However, the stiffness of the RAP elements more than accounts for the reduction in strength resulting from installation for both the static and seismic conditions.

Conversely, the improvement factors greater than 2 below a depth of 10 m (average of 2.7) are expected in the more granular material at these depths and in line with prior observations (Wissmann et al. 2015, Saftner et al. 2017, Vera-Grunauer et al. 2017, Amoroso et al. 2019, Rollins et al. 2021).

Third, some improvement below the tip of the elements is also observed. Between a depth of 11.5 m and 12.2 m (about 3 pier diameters), an average improvement factor of 2.2 is observed. This demonstrates the effects of the vertical compaction energy and the ability to densify soils below the tips of the elements.

Fourth, below the improvement seen from the pier tip at a depth of 12.2 m, the average "improvement factor" is 1.0, when excluding the material around 17 m where both post-CPT soundings showed improvement, which is indicative of a change in soil type. As these are the depths in which no improvement is expected, the 1.0 improvement factor provides verification that the pre- and post-CPTs are sufficiently similar to be used for validation.

4.3 *Design validation*

Demonstrating an improvement in the relative density through post-CPT testing is not sufficient to validate the design as the results should also be used to update the design with respect to settlement. Critical to this step is understanding that CPT soundings only measure one of the three mechanisms of improvement (densification). The other two mechanisms (Ko increase and pier stiffness) should still be considered. Note that dilatometer testing can measure Ko increase if used for post-verification testing, and the results used directly for design verification. Otherwise, relying on the previously referenced studies in similar soil conditions is adequate.

The factors of safety against liquefaction plots are shown in Figure 7a and 8a (Turbine A and B respectively). Note that the plots considered the turbine embedment depths of 3.6 m and 4.1 m, respectively, which is why no Factors of Safety are shown above these depths. Both figures show a significant increase in the FS, rendering much of the profile no longer susceptible to liquefaction.

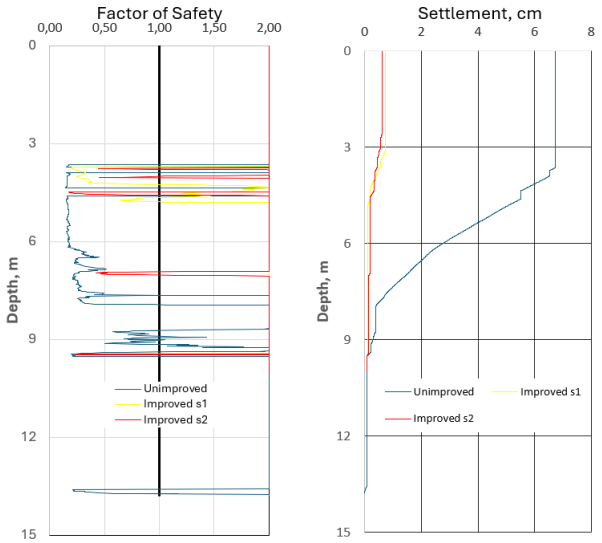

Figure 7. Turbine A - Factor of Safety against liquefaction (a, left); liquefaction induced settlement (b, right).

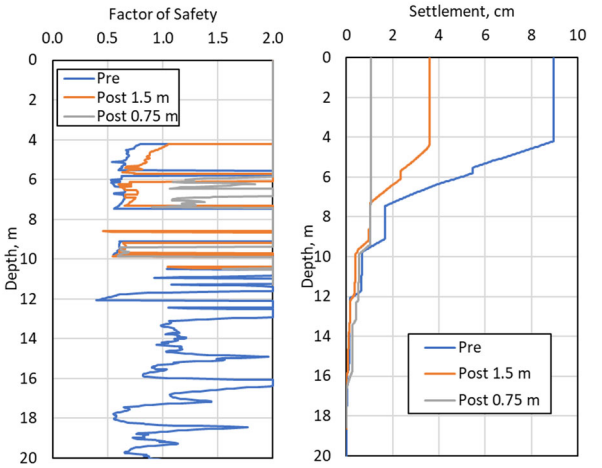

Figure 8. Turbine B - Factor of Safety against liquefaction (a, left); liquefaction induced settlement (b, right).

The liquefaction-induced settlements verses depth are shown in Figures 7b and 8b. These settlements are calculated directly from the post-installation CPTs and while considering a Ko increase.

Observe that the liquefaction-induced settlement was reduced from 7.5 cm to 0.5cm for Turbine A and from about 9 cm to less than 4.0 cm for Turbine B. These values easily meet the performance criteria of 3mm/m differential settlement for the static and seismic conditions.

In summary, the results of the post-validation testing demonstrated that the RAP elements successfully improved the ground and that the ground improvement design will function as designed.

5 CONCLUSION

The projects described in the article offer a helpful approach that can be used not only in areas like VSZ and NMSZ, but also in other earthquake-prone regions in Europe and the USA. They show how ground improvement methods, especially Rammed Aggregate Piers, can reduce performance risks to structures resulting from earthquake induced ground motions. As shown here, ground improvement can address several problems at once, such as liquefaction, settlement, and low bearing capacity, leading to safe and cost-effective designs for important infrastructure. As the demand for renewable infrastructure grows in regions that pose particular performance risks, ground improvement will become increasingly more important in providing resilient and affordable foundations that both satisfy performance criteria and meet accelerated construction schedules.

6 REFERENCES

Amoroso, S., Rollins, K.M., Andersen, P., Gottardi, G., Tonni, L., Garcia Martinez, M.F., Wissmann, K., Minarelli, L.2019. "Full-scale testing of liquefaction mitigation using rammed aggregate piers in silty sands." Earthquake Geotechnical Engineering for Protection and Development of Environment and Constructions. Associazione Geotecnica Italiana. Rome, Italy. 656 – 663.

Amoroso, S., et al. 2020. "Blast-induced liquefaction in silty sands for full-scale testing of ground improvement methods: Insights from a multi-disciplinary study". Engineering Geology. 265 (Feb): 105437.

Amoroso, S., Rollins, K.M., Minarelli, L., Monaco, P., Wissmann, K.2024. "Improved liquefaction resistance with rammed aggregate piers resulting from increased earth pressure coefficient and density". ASCE Journal of Geotechnical and Geoenvironmental Engineering. Vol 150, No 6.

Cetin et al., 2009. Probabilistic model for assessment of cyclically induced reconsolidation (volumetric) strains. ASCE Journal of Geotechnical and Geoenvironemental Engineering. Vol 135, No 3, pp 387-398.

Duncan J.M. and S.G. Wright. 2005. Soil Strength and Slope Stability. Wiley. Hoboken, NJ.

Harada, K., R.P. Orense, K. Ishihara, and J. Mukai. 2010. "Lateral Stress Effects on Liquefaction Resistance Correlations." Bulletin of the New Zealand Society for Earthquake Engineering.

Highway Innovative Technology Evaluation Center (HITEC). 2007. Evaluation of Geopier Rammed Aggregate Piers by Geopier Foundation Company – Final Report. American Society of Civil Engineers. Reston, VA.

Majchrzak, M., T. Farrell, and B. Metcalfe. 2009. "Innovative Soil Reinforcement Method to Control Static and Seismic Settlements." ADSC. American Society of Civil Engineers. Orlando FL.

Rollins K.M., Amoroso S., Andersen P., Tonni L., and K. Wissmann. 2021. "Liquefaction Mitigation of Silty Sands Using Rammed Aggregate Piers Based on Blast-Induced Liquefaction Testing". Journal of Geotechnical and Geoenvironmental Engineering. Volume 147, Issue 9.

Robertson, P.K. and K.L Cabal. 2009. Guide to Cone Penetration Testing for Geo-Environmental Engineering. 2nd Ed. Gregg Drilling and Testing, Inc. Signal Hill, CA.

Robertson, P.K. and Wride, C.E., 1998. Cyclic Liquefaction and its Evaluation based on the CPT. Canadian Geotechnical Journal. Volume 35, August.

Saftner, D., J. Zheng, R. Green, and K.J. Wissmann. 2017. "Rammed Aggregate Pier Installation Effect on Soil Properties." Institute for Civil Engineers. ICE. 2017.

Salgado, R., Boulanger, R.W., Mitchell, J.K., 1997. Lateral Stress Effects on CPT Liquefaction Resistance Correlations. Journal of Geotechnical and Environmental Engineering, Volume 123, Issue 8.

Smith, M.E. and Wissmann, K.J., 2017. Ground Improvement Reinforcement Mechanisms Determined for the Mw7.8 Muisne, Ecuador, Earthquake. Geotechnical Earthquake Engineering and Soil Dynamics V.

Vera-Grunauer, X., K.J. Wissmann, M.E. Smith, and J. Arroyo-Esqueda. 2017. "Liquefaction Mitigation of Silty Sand and Sand Silt Soils with RAPs." Sociedad Mexicana de Ingenieria Geotechnica A.C. CDMX. Mexico.

Vera-Grunauer, X.F., Lopez-Zhindon, S., Ordoñez-Rendon, J., Chavez-Abril, M.A., 2019. Liquefaction Case Histories after the 2016 Megathrust Pedernales Earthquake in Ecuador. 7th International Conference on Earthquake Geotechnical Engineering.

White, D. J., H. T. Pham, and K. K. Hoevelkamp. 2007. "Support mechanisms of rammed aggregate piers. I: Experimental results." J. Geotech. Geoenviron. Eng. 133 (12): 1503-1512.

White, D. J., M. T. Sulieman, H. T. Pham, and J. Bigelow. 2002. Constitutive equations for aggregates used in geopier foundation construction. Ames, IA: Iowa State University.

Wissmann, K. 2022. Bearing Capacity of Geopier Supported Foundation Systems. Geopier Technical Bulletin No. 2. Geopier. Davidson, NC.

Wissmann K., Ballegooy S.V., Metcalfe B.C., Dismuke J.N., and C.K. Anderson. 2015. "Rammed Aggregate Pier Ground Improvement as Liquefaction Mitigation Method in Sandy and Silty Soils". Proceedings of the 6th International Conference on Earthquake Geotechnical Engineering. Christchurch, New Zealand.

Yasuhara, K. 1994.Postcyclic undrained shear strength for cohesive soils. Journal of Geotech. Eng., ASCE, 120 (11), 1961-1979.

Youd, T.L. et al. (2001). "Liquefaction resistance of soils: Summary report from the 1996 NCEER and 1998 NCEER/NSF workshops on evaluation of liquefaction resistance of soils," Journal of Geotechnical and Geoenvironmental Engineering, ASCE, 127(10), 817-833.

Zalachoris G., Zekkos D., Yerro A., Bowers G.A., and K.J. Wissmann. 2023. "3D Numerical Assessment of Rammed Aggregate Pier Performance under Dynamic Loading in Liquefiable Soils". Journal of Geotechnical and Geoenvironmental Engineering. Volume 149. Issue 3.

Zhang, G., Robertson, P.K., Brachman, R.W.I., 2002. Estimating liquefaction-induced ground settlements from CPT for level ground. Can. Geotech. J. 39, 1168-1180.